# Off-axis Sawteeth and Double-tearing Reconnection in Reversed Magnetic Shear Plasmas in TFTR

Z. Chang, W. Park, E. D. Fredrickson, Et al

in RECEIVED

JUN 24 1996

OSTI

Off-axis sawteeth are often observed in reversed magnetic shear plasmas when the minimum safety factor q is near or below 2. Fluctuations with $m/n = 2/1$ (m and n are the poloidal and toroidal mode numbers) appear before and after the crashes. Detailed comparison has been made between the measured Te profile evolution during the crash and a nonlinear numerical magnetohydrodynamics (MHD) simulation. The good agreement between the observation and simulation indicates that the off-axis sawteeth are due to a double-tearing magnetic reconnection process.

## DISCLAIMER

# Off-axis Sawteeth and Double-tearing Reconnection in Reversed Magnetic Shear Plasmas in TFTR

Z. Chang[1], W. Park[1], E. D. Fredrickson[1], S. H. Batha[2], M. G. Bell[1], R. Bell[1],

R. V. Budny[1], C. E. Bush[1], A. Janos[1], F. M. Levinton[2], K. M. McGuire[1], H. Park[1],

S. A. Sabbagh[3], G. L. Schmidt[1], S. D. Scott[1], E. J. Synakowski[1], H. Takahashi[1],

G. Taylor[1], and M. C. Zarnstorff[1]

[1] *Plasma Physics Laboratory, Princeton University, Princeton, NJ 08543*

[2] *Fusion Physics and Technology, Torrance, CA*

[3] *Columbia University, New York, NY*

(April 25, 1996)

## Abstract

Off-axis sawteeth are often observed in reversed magnetic shear plasmas when the minimum safety factor $q$ is near or below 2. Fluctuations with $m/n = 2/1$ ($m$ and $n$ are the poloidal and toroidal mode numbers) appear before and after the crashes. Detailed comparison has been made between the measured $T_e$ profile evolution during the crash and a nonlinear numerical magnetohydrodynamics (MHD) simulation. The good agreement between the observation and simulation indicates that the off-axis sawteeth are due to a double-tearing magnetic reconnection process.

Sawtooth MHD activity is commonly observed in tokamak experiments when the central safety factor $q$ is below 1 and rises monotonically with minor radius. In recent reversed magnetic shear (RS) experiments in the Tokamak Fusion Test Reactor (TFTR), another kind of sawtooth activity has been observed in plasmas with nonmonotonic $q$ profiles or hollow plasma current profiles when $q(r) > 1$. Understanding these $q > 1$ sawteeth is important not only because it can help us explore magnetic reconnection physics, but also because it is closely related to present and future advanced tokamak research.

Figure 1 shows a typical RS discharge. The RS configuration is obtained by combining an early energetic neutral beam injection (prelude phase) and large current ramp rate [1]. During the high power heating phase, this discharge developed an enhanced reversed shear (ERS [1]) mode. Two sawtooth events are observed after the main heating phase. One is at 3.3 sec, during the low beam power phase, and another at 3.75 sec, in the post-beam phase. The $q$ profile up to $t = 2.5sec$ is from Motional Stark Effect (MSE) polarimetry [2,3] measurement. After that, the $q$ profile is calculated by a transport code TRANSP [4] based on measured plasma profiles. The minimum $q$ ($q_{min}$) and central $q$ ($q_0$) are shown in Fig. 1(b), which indicates that the $q$ profile is reversed, i.e., $q_0 > q_{min}$. The sawteeth occur when the $q_{min}$ passes 2. They can be easily seen on the electron temperature evolution [Fig. 1(c)] measured by an electron-cyclotron-emission (ECE) diagnostic system. Their effects or correlated changes can also be observed in ion temperature, plasma rotation and electron density, Fig. 1(d)-(f). Correlated negative spikes in plasma loop voltage and changes in plasma radius are also observed. These sawteeth can appear in the non-enhanced RS phase as well as in the ERS phase. The plasma composition (deuterium-only or deuterium-tritium) does not alter the sawtooth activity.

Two types of $q(r) > 1$ sawteeth are observed on TFTR: an off-axis sawtooth, which is observed most commonly, and an on-axis sawtooth. Figure 2(a) (the first sawtooth in Fig. 1) shows the $T_e$ fluctuation and profile behavior of the off-axis sawtooth. The central $T_e$ does not immediately crash at the sawtooth event. We call this an "annular-crash". Precursors around the inversion region are often observed. Mode analysis using magnetic coils and two

2

toroidally-separated ECE systems [13] shows that the precursor mode has a toroidal mode number $n = 1$. The poloidal mode number is even from the phase analysis of the ECE data. The precursor (and postcursor when they exist) modes are identified as $m/n = 2/1$ modes since the $q$ value near the MHD region is about 2, see Fig. 3(a). (Note that the external magnetic measurement usually indicates $m \simeq nq_a$ due to toroidal coupling.) Figure. 2(b) shows the second type sawtooth (similar to the second sawtooth in Fig. 1). The central $T_e$ crashes on nearly the same time scale ($20 - 50 \ \mu s$) as the off axis $T_e$ crash. We call this case a "core-crash". The $m/n = 2/1$ precursor mode occupies a larger region in the core-crash cases. As we will show later, this is consistent with the fact that the core-crash case has a larger region between the two $q = 2$ surfaces.

These observations (off-axis feature, fast time scale and the multiple rational surfaces in the reversed $q$ profile) suggest that the crashes are due to fast magnetic field line reconnection, analogous to a $q = 1$ reconnection. We find that the Kadomtsev model [5] applied to a double-tearing reconnection [6,7] qualitatively agrees with the observations. This theory assumes that for a reversed shear magnetic configuration, two pairs of $m/n = 2/1$ islands develop at the two $q = 2$ surfaces and reconnect with a time scale much faster than the single tearing case. Figure 3 shows the calculated changes of $q(r)$, helical magnetic flux $\psi$ and $T_e$ before (from the measurement) and after the reconnection for the annular-crash shown in Fig. 2(a). Here, in a cylindrical geometry we have $\psi(r) \propto \int_0^r (1/q - n/m) r dr$. The mixing region is determined by the width of the two $q = 2$ surfaces and $q$ profile. The $q$ profile within the mixing region relaxes to $\geq 2$ after the reconnection. In large annular-crash sawteeth, changes in the magnetic pitch angles are observed on the MSE channels in the vicinity of the sawtooth region, indicating an increase of $q$ in the $q_{min}$ region and decrease of $q$ in the mixing region. To date, only the changes in the inner mixing region ($r < r_{s1}$) have been observed. The $T_e$ profile after the reconnection is usually strongly inverted due to the assumption of no transport during the reconnection. When the $q < 2$ region increases, the inner mixing radius becomes smaller and smaller. Eventually, when $\psi(r_{s2}) \geq \psi(r = 0) = 0$, or $\int_0^{r_{s2}} (1/q - n/m) r dr \geq 0$, the reconnection will cover the center. A core-crash is then

3

expected.

For a more detailed study, we used a nonlinear 3D MHD code *MH3D* [8] to follow the double-tearing reconnection process. Measured $T_e(r)$ and $q(r)$ profiles before a sawtooth are used as initial conditions. The nonlinear development of the double-tearing instability is then followed self-consistently. The dominant behavior is the fast magnetic reconnection and subsequent $T_e$ equalization along the reconnected field lines. The large parallel electron thermal conductivity is accurately treated using the technique of artificial parallel sound wave [9]. We first study the core-crash case of the second sawtooth in Fig. 1. For this relatively low beta case (volume averaged $\epsilon\beta_p \sim 0.03$), 2D simulation gives a similar global behavior as 3D toroidal simulation which was carried out part way to check whether 3D toroidal effects are important. (For high-$\beta$ cases, 3D toroidal effects often dominate the global behavior [8].) The Lundquist number $S \sim 10^4$ and $10^5$ are used to ensure that the global behavior is not sensitive to the Lundquist number used which is much lower than the experimental value of $S \sim 10^8$. Figure 4 shows the 2D simulation results using the plasma parameters for the core-crash case of the second sawtooth in Fig. 1. Four phases can be distinguished. (a) The early growth phase. (b) The double-tearing reconnection phase. (c) The central temperature (pressure) collapse phase. (d) The final temperature (pressure) equalization phase. The left column of Fig. 4 displays the contours of the magnetic flux on a plasma cross-section. The right column shows the corresponding $T_e$ profiles in *minor radius*. For comparison, the $T_e$ profile along the $\theta = 0°$ (*O* point of the inner island) is plotted on the right side. The $T_e$ profile along the $\theta = 90°$ (*O* point of the outer island) is on the left side. At the early phase (a) the two pairs of islands are well separated. It is probably responsible for the observed 2/1 precursor. At the reconnection phase (b), the inner hot islands move out through the $X$ points of the outer cold islands. At the same time the outer cold islands move in through the $X$ points of the inner hot islands. Note that since the reconnection time is much faster than the perpendicular transport time, the temperature profile around the $0°$ section is higher than the temperature around the $90°$ section, see Fig. 4(b) and (c). A relative "hot spot" appears at the outer mixing radius at the later stage of the reconnection,

4

see Fig. 4(d). The reconnection time scale during the phases shown above corresponds to a Sweet-Parker scaling [10], $\tau_A^{1/2}\tau_R^{1/2}$, which is $\sim 1msec$ for the experimental parameters. [11] While the experimental evolution time during the phase corresponding to (d) (see the next paragraph) roughly agrees with this, the experimental crash time corresponding to phases (b) and (c) is about an order of magnitude faster, possibly due to turbulence in the reconnection layer [12], which is not intended to be resolved in our calculation. What is contained in the global simulation is that the reconnection is much faster than the usual nonlinear tearing mode time scale ($\propto \tau_R$) of $\sim 100msec$ for the experimental parameters studied here.

Good agreement was found between the measured $T_e$ profile evolution and the double-tearing reconnection simulation described above. The fast $T_e$ profile evolution data are obtained from the two 20-channel grating polychromator ECE arrays [13]. The sampling rate is 500 $kHz$, which gives a 2 $\mu sec$ time resolution. The channel-to-channel separation is about 5-6 $cm$. The radial spatial resolution for each channel is about 3 $cm$. The two ECE arrays are toroidally separated by 126°, Fig. 5(a). For $m = 2$ modes, they are effectively simultaneously measuring two $T_e$ profiles separated 63° poloidally. Therefore, if one of the ECE arrays happens to catch the crash phase around the $O$-point region of the cold-island (*cf.* the 90° section in Fig. 4) the other ECE array will measure the $T_e$ profile near the central region of the hot-island (around the 0° section in Fig. 4). The evolution of the second core-crash sawtooth in Fig. 1 is shown in Fig. 5(c)-(f). Since the crash phase is much shorter ($\lesssim 30\mu s$) than the precursor oscillation period ($\gtrsim 2.5ms$), the two ECE arrays measure the sawtooth crash with nearly fixed phase with respect to the island locations. Before the sawtooth precursor the $T_e$ profiles from both ECE arrays are nearly identical. Just before the crash [$t = t_1$ in Fig. 5(c) and (d)] a flat spot with $T_e \sim 3.8\ keV$ starts to form and expand. It locates at the inner $q = 2$ surface according to the $q$ profile in Fig. 5(b), which indicates that the ECE2 is measuring the hot island region [*cf.* 0° profile of Fig. 4(a)]. During the crash phase the hot island grows rapidly outward to the outer $q = 2$ region. The central $T_e$ also starts to drop, see $t_2$ profile in Fig. 5(d) and compare

5

with Fig. 4(b). As the reconnection continues to the core the central $T_e$ collapses. The $T_e$ profile from ECE2 becomes hollow as predicted by the simulation, see $t_3$ profile in Fig. 5(d) and compare with Fig. 4(c). After the crash, the $T_e$ profile starts to flatten, see $t_4$ profile in Fig. 5(d) and compare with Fig. 4(d). The $T_e$ evolution from the ECE1 array shows a very different pattern with respect to ECE2. As shown in Fig. 5(e) and (f), a 2 $keV$ cold island develops at the outer $q = 2$ surface. The $T_e$ profiles in each stage agrees well with the simulation shown as the 90° section in Fig. 4. In annular-crash cases, similar good agreement on the $T_e$ evolution has also been found between the ECE measurement and the double-tearing simulation.

Experimentally, we also observed cases where large magnetic islands remain after a fast crash phase followed by a strong 2/1 postcursor. This phenomenon may be understood from the double-tearing model if the fast reconnection is incomplete. For example, the fast reconnection stops at phase (b) in Fig. 4.

Occasionally, off-axis sawteeth with a $m/n = 3/1$ island precursor are observed in RS plasmas. They happened as $q_{min}$ passes 3. This event can also be explained by the double-tearing reconnection model if 3/1 islands are introduced. [7]

Identification of the two magnetic islands in the precursor is usually difficult. This is mainly due to the finite spacing (5-6 cm) between the ECE channels and the very different spatial structure of the double-tearing perturbation. Numerical simulation shows that the $\delta T_e$ phase inversion feature, which is usually used to identify magnetic islands, becomes very weak in the double-tearing case. Nevertheless, the $\delta T_e$ phase inversions on both $q = 2$ surfaces were observed when islands were large, as in Fig. 2(b). In higher-$\beta$ RS/ERS discharges, the double-tearing reconnection mechanism studied here sometimes causes disruptions. 3D simulations also show similar behavior.

A different theoretical model [14], based on ballooning mode destabilization in the presence of a single large island, has been proposed to explain the off-axis sawteeth observed in shear reversal experiments in Tore-Supra tokamak. We do not believe this model can explain the detailed profile evolution observed from the two sets of ECE data in TFTR.

6

As in $q = 1$ sawtooth studies, two major questions remain to be answered. First, how does the measured $q$ profile change after the sawtooth? Ongoing improvements to the MSE diagnostic and analysis techniques may allow this question to be answered in the future. Second, how is the double-tearing mode destabilized? A statistical data analysis shows that off-axis 2/1 sawteeth occur in nearly half the discharges in TFTR RS experiments during the 1995 run. In many cases the discharges with and without sawteeth are very similar in terms of the measured plasma parameters, including $q(r)$. Statistical data from local density and temperature and their gradients show no clear "parameter boundary" between the sawtoothing and non-sawtoothing discharges. Also it is found that the precursor activity varies dramatically in similar sawtoothing discharges. There is more than an order of magnitude difference in precursor time and growth rate.

In conclusion, off-axis sawteeth have been observed in TFTR reversed shear experiments. They usually have $m/n = 2/1$ MHD precursors and occur after $q_{min}$ crosses 2. The crash time ($\sim 20 - 40\mu s$) and repetition time ($\sim 100 - 400\ ms$) are similar to the $q = 1$ sawteeth in monotonic $q$ profile plasmas. The detailed comparison between the $T_e$ profile evolution and the MHD simulation confirms, for the first time, that the observed off-axis sawteeth are due to the double-tearing magnetic reconnection process.

# REFERENCES

[1] F. M. Levinton *et al.*, Phys. Rev. Lett. **75**, 4417 (1995).

[2] F. M. Levinton *et al.*, Phys. Rev. Lett. **63**, 2060 (1989).

[3] F. M. Levinton, Rev. Sci. Instrum. **63**, 5157 (1992).

[4] R. V. Budny, Nucl. Fusion **34**, 1247 (1994) and references therein.

[5] B. B. Kadomtsev, Fiz. Plazmy **1**, 710 (1975) [Sov. J. Plasma Phys. **1**, 389 (1975)].

[6] R. B. White, D. A. Monticello, M. N. Rosenbluth and B. V. Waddell, in *Plasma Physics and Controlled Nuclear Fusion Research 1977* (IAEA, Vienna, 1977), Vol. 1, p. 569.

[7] B. Carreras, H. R. Hicks and B. V. Waddell, Nucl. Fusion **19**, 583 (1979).

[8] W. Park, D. A. Monticello, E. Fredrickson, K. McGuire, Phys. Fluids B **3**, 507 (1991).

[9] W. Park, D. A. Monticello, H. Strauss and J. Manickam, Phys. Fluids **29**, 1171 (1986).

[10] E. N. Parker, J. Geophys. Res. **62**, 509 (1957).

[11] W. Park, D. A. Monticello and R. B. White, Phys. Fluids **27**, 137 (1984).

[12] J. F. Drake, R. G. Kleva and M. E. Mandt, Phys. Rev. Lett. **73**, 1251 (1994).

[13] A. Janos *et al.*, Rev. Sci. Instrum. **66**, 668 (1995).

[14] D. Edery *et al.*, in *Proceedings of the 22$^{nd}$ European Physical Society Conference on Controlled Fusion and Plasma Physics, Bournemouth, 1995*, edited by B. E. Keen, et al., Vol. IV, p. IV-065.

# FIGURES

FIG. 1. Two sawtooth crashes were observed in this reversed shear discharge. One at 3.3 sec, the other at 3.72 sec. They occur after the $q_{min}$ passes 2 (b). The correlated changes can be seen on $T_e$ in (c), $T_i$ in (d), $V_\phi$ in (e) and $n_e$ in (f).

FIG. 2. Temperature fluctuations (left) and profile changes (right) for two kinds of sawtooth crashes. (a) Annular crash. Precursor with $m/n = 2/1$ is observed. The fast crash only affects the annular region. (b) Core crash. The 2/1 precursor occupies a larger region. $\delta T_e$ phase inversions can be seen on both sides of the precursor.

FIG. 3. Predicted profile changes after (dashed curves) the a magnetic reconnection from the Kadomtsev model. The initial $q$ and $T_e$ profiles (solid curves) are taken from the first sawtooth in Fig. 1.

FIG. 4. Numerical simulation of a double-tearing reconnection. The left column shows the contours of the magnetic flux. The corresponding $T_e$ profiles (in minor radius) for $\theta = 0°$ and $90°$ sections are shown on the right. Four phases can be distinguished. (a) The early growth phase. (b) The double-tearing reconnection phase. (c) The central temperature collapse phase. (d) The final temperature equalization phase.

FIG. 5. (a) The two ECE systems are toroidally separated by $126°$. (b) The $q$ profile before the second core-crash sawtooth in the discharge shown in Fig. 1. The $T_e$ contour plot (c) and profiles (d) show the $T_e$ evolution measured from the ECE2 array. The $T_e$ evolution in the same time window measured from the ECE1 array is shown in (e) and (f). The basic feature is the hot island moves out and cold island moves in, which is in good agreement with the numerical simulation (cf. Fig. 4).
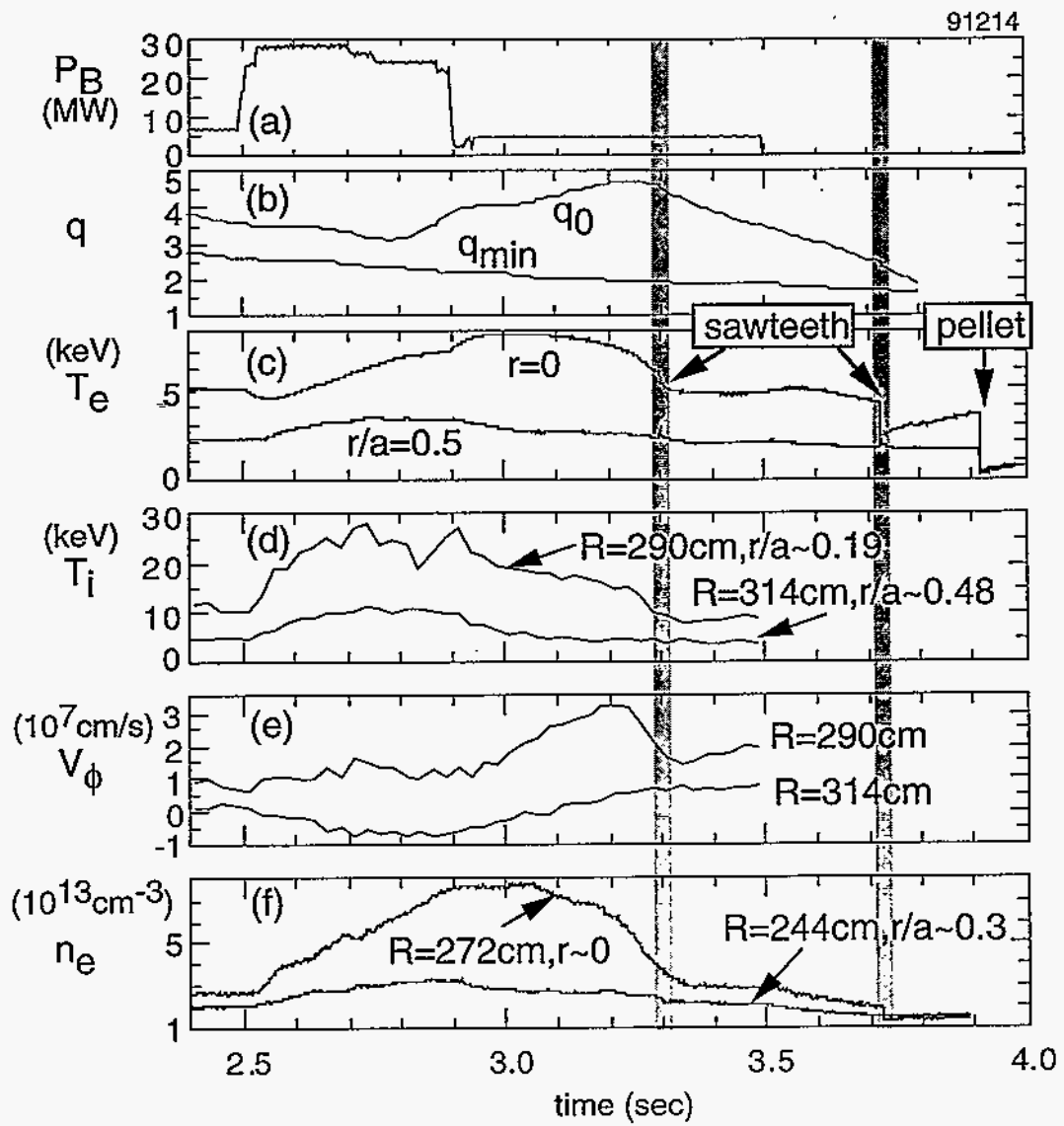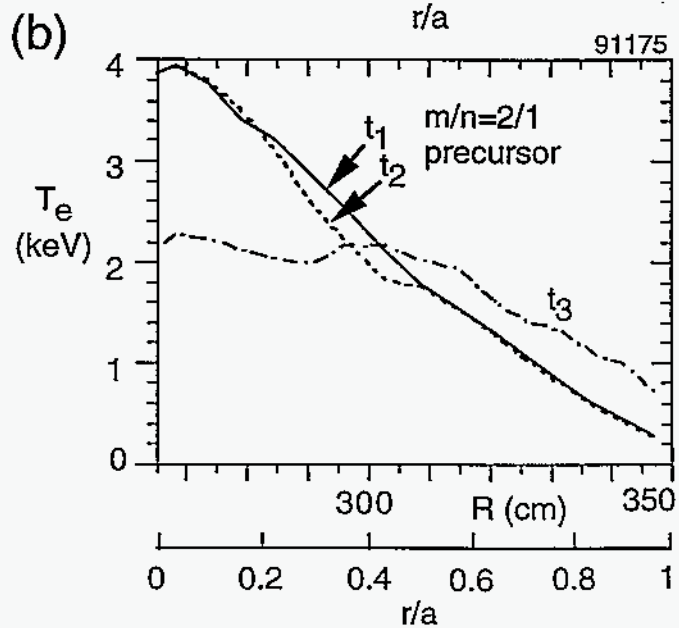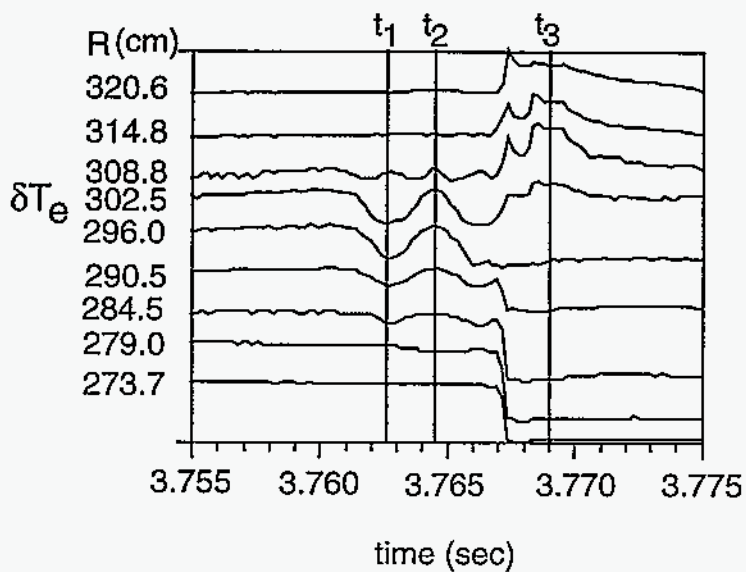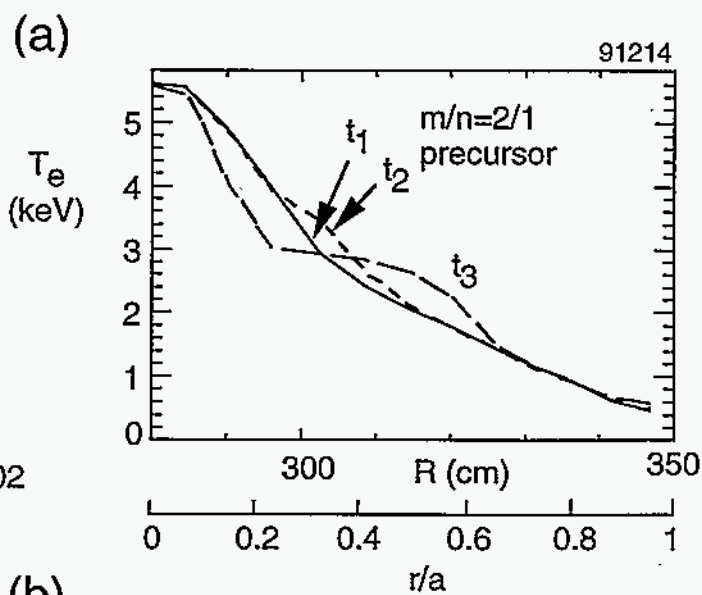
Fig. 1.

Fig. 2

(a) 91214

t = 3.3 sec

(b)

Fig. 3

FIG. 4.

(a) ECE2 φ TFTR top view ECE1

(b) 91214 t=3.7 sec q R(cm)

(c) 20 μs $t_1$ $t_2$ $t_3$ $t_4$ 350 (cm) 300 R axis 250 ECE2 3.7274 3.7275 3.7276 3.7277

(d) (keV) hot island $t_1$ $t_2$ $T_e$ $t_3$ $t_4$ 4ms before sawtooth ECE2

(e) 350 (cm) 300 R 250 ECE1 3.7274 3.7275 3.7276 3.7277 Time (sec)

(f) (keV) 4ms before sawtooth $t_1$ $t_2$ $T_e$ $t_3$ $t_4$ cold island ECE1 250 300 350 R (cm)

Fig. 5